ICONHIC 2016
1st International Conference on Natural Hazards & Infrastructure
28-30 June, 2016, Chania, Greece

# Steel sheet-pile quay-walls: seismic analysis

A. Zafeirakos, E. Garini, G. Gazetas[1]
*National Technical University of Athens*

## ABSTRACT

The paper investigates the performance of a typical anchored steel sheet-pile (SSP) quay-wall against seismic motions of various intensities. The SSP wall has a "free" height of 18 m and it supports medium-dense to dense, non-liquefiable sandy soils. The wall is subjected to two levels of seismic excitation with respect to the PGA at the rock-outcrop level, namely 0.15 g and 0.5 g. The investigation is performed: (i) according to long-established procedures that combine pseudo-static limit equilibrium method (pLEM) with the beam-on-Winkler-foundation (BWF), and (ii) by means of advanced finite element (FE) analysis with use of two commercially available codes (ABAQUS, PLAXIS). It is shown that the simplified methodology, which works in conjunction with the Mononobe-Okabe (MO) method, leads to results for the structural distress that can be significantly larger than those computed by the FE analysis. The advantage of performing detailed numerical analysis for such complex soil-structure interaction problems is furthermore demonstrated by its ability to capture well the physical phenomena, leading to similar results despite the sensitivity to the soil constitutive model. Needless to say, the mere possibility of liquefaction must be excluded or mitigated by suitable soil improvement.

*Keywords: anchored sheet-pile wall, seismic design, Mononobe-Okabe, numerical analysis*

## INTRODUCTION

Port facilities have often suffered damage in strong earthquakes, causing among other problems disruptions of post-earthquake emergency operations with serious economic consequences for the stricken regions. The numerous small and large failures of caisson type quay-walls in the port of Kobe during the 1995 earthquake, complemented the deformations/failures of the anchored sheet-pile walls of earlier seismic episodes in Japan (e.g., in the Niigata 1964 [Kawakami & Asada (1966)] and the Tokachi-oki 1968 [Hayashi & Katayama (1970)] earthquakes).

Anchored SSP walls (crudely sketched in Fig. 1) are often used as retaining structures in wharves and quays thanks mainly to their easy installation, while the soft or loose soils that usually underline such waterfront structures could hardly support the additional weight of gravity concrete walls. Thus, in many cases such walls are cheaper than gravity walls on piles. Consequently, a measurable portion of quay-walls are anchored sheet-piles and, thereby, many of the reported quay-walls seismic failures are of such walls [e.g. Agbabian Associates (1980), Dennehy (1985)]. The following conclusions emerge from a study of the performance of anchored bulkheads in very strong earthquake shaking:

1. Most of the observed earthquake failures have resulted from large-scale liquefaction of loose cohesionless soils mainly in the backfill but sometimes in the supporting foundation soil. Such soils may not be rare in port and harbor facility sites.

[1] Corresponding Author: G. Gazetas, *National Technical University of Athens*, gazetas@central.ntua.gr

2. Another frequent but not as dramatic type anchored bulkhead damage takes the form of excessive permanent seaward "bulging" and tilting of the sheet-pile wall, accompanied by excessive movement of the anchor block or plate relative to the surrounding soil; such an anchor movement manifests itself in the form of settlement of the soil and cracking of the concrete apron directly behind the anchor. Apparently, such failures are due either to inadequate passive resistance against the anchor wall, or to insufficient strength of the main SSP wall, or both.
3. Development of detrimental excess pore-water pressures in the backfill next to the wall, once thought to be a contributor to large deformations and failure, is now recognized as unlikely to occur when seaward bulging takes place [Dakoulas & Gazetas (2008), Towhata et al. (1996)].
These observations suggest that anchored bulkheads must be properly designed against strong shaking, just as should caisson and other type of walls.

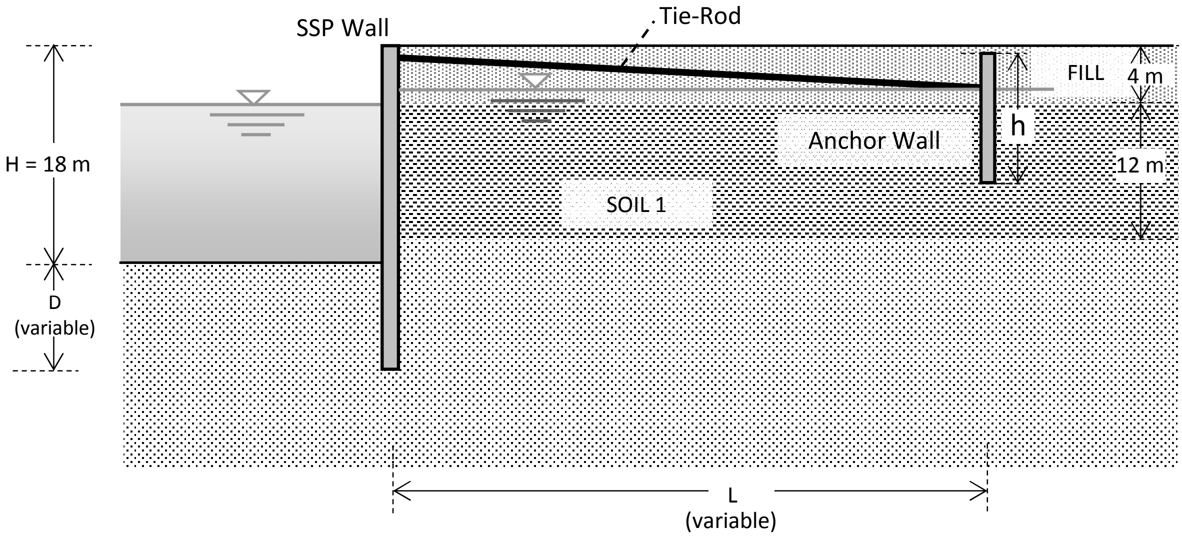


**Figure 1.** Example SSP wall used in this study

## ON THE STATE-OF-PRACTICE SEISMIC DESIGN PROCEDURES

The difficulty of providing a comprehensive rigorous analytical method arises from several factors: the complicated wave diffraction pattern due to "ground-step" geometry; the presence of two different but interconnected structural elements in contact with the soil; the inevitably nonlinear hysteretic behavior of soil in strong shaking, often including pore-pressure buildup and degradation, both in front and behind the main wall; the no-tension behavior of the soil-SSP wall interface; the presence of radiation damping effects due to stress waves propagating away from the wall in the backfill and in the foundation ─ let alone the hydrodynamic effects on both sides of the wall. Before the advent of reliable and relatively user friendly FE and FD codes which could properly handle all these phenomena, pseudo-static simplified procedures were (and are still) used in practice. Specifically:

(1) ***Pseudo-Static Limit Equilibrium Methods***, (pLEM) determine dynamic lateral earth pressures with the Mononobe-Okabe analysis. Differences among the several variants of the method [e.g. Ebeling and Morrison (1992), JSCE (1980), Richards and Elms (1979)] arise primarily from the assumed point of application of the resultant active and passive forces $F_{AE}$ and $F_{PE}$ (on the two sides of the SSP wall), the handling of the water, and the partial factors of safety introduced in the design. Among other problems, MO method produces seismic earth pressure active and passive coefficients, $K_{AE}$ and $K_{PE}$, that are too sensitive to (large values of) the effective ("driving") acceleration ── in disagreement with rigorous FE analyses and field observations during many earthquakes.

(2) ***Beam-on-Winkler-Foundation*** [BWF] modeling treats the sheet-pile wall just as a pile foundation, with suitable one-sided plane-strain linear Winkler springs (or non-linear p–y reaction "springs") on both the

active and passive sides of the wall, with an elasto-plastic support for the anchor. Two 1-D shear beams are attached to the ends of the springs and transmit the seismic motion to the system. The kinematic response that is ensuing could reproduce the flexural response of the wall with reasonable accuracy, but only for very small levels of excitation. When the acceleration level is high enough to induce wedge-type failure mechanisms and the anchor is activated passively, the results would not necessarily be reliable.

(3) ***Hybrid procedures***, combining the BWF with the pLEM methods have been perhaps the most widely used in practice. Because of the reliance of these methods on the MO active earth pressures they usually lead to very conservative results as will be shown later.

With the advent of reliable and experimentally validated FE codes the simplified methods are slowly becoming redundant. Their use may lead to unrealistically exaggerated bending moments for the wall [e.g. Al Atik and Sitar (2010)] and distance of the anchoring point, as it will be demonstrated below.

## COMPARATIVE STUDY

The 32 m long sheet-pile wall (18 m free and 14 m embedded), shown in Fig. 1, is analyzed dynamically with the finite element codes ABAQUS and PLAXIS. The wall is embedded into a dense sandy layer, while the backfill soil comprises a medium dense (but not liquefiable) silty sand overlain by a conhesionless fill. The strength and stiffness parameters of the three layers are given in Table 1 and are typical of those encountered in harbors. The cross-sections of the walls have the forms of Fig. 1 with parametrically varying their dimensions and thickness. For the main SSP wall, the rigidity ranges from $EI \approx 1 \times 10^6$ to $2.3 \times 10^6$ kNm$^2$/m, while the ultimate moment capacity from $M_{ult} \approx 4000$ kNm/m to 8000 kNm/m. The distance of the anchor wall to the main SSP wall (which is the length of the tie-rod), $L_{anch} = 45$ m to 55 m.

**Table 1.** Soil parameters.

| | ***c*** **(kPa)** | ***φ*** **(deg)** | ***E*** **(MPa)** |
|---|---|---|---|
| **Fill** | 1 | 32.5 | 100 |
| **Soil 1** | 8 | 35 | 200 |
| **Soil 2** | 10 | 37.5 | 300 |

A description of the two FE models is given below:

*PLAXIS*: The FE mesh (Fig. 2) consists of triangular 6-node elements. The geometry has been mirrored, in order to (*a)* ameliorate the lateral boundary effects, and (*b*) examine the effect of the inherent asymmetry of the accelerogram (“polarity” effect) in a single dynamic analysis.

The maximum finite element size is deliberately chosen to be about 10 times smaller than the minimum wavelength of significance, thus avoiding spurious filtering effects. The adhesion between the soil and SSP wall is taken into account by adding positive and negative interface elements between the wall and the soil. Interface strength value of $R_{inter} = 0.67$ is considered.

For the undrained effective stress analysis, the Hardening-Soil Small [HSS] model is used [PLAXIS manual, (2012)]. This advanced model is able to treat small-strain stiffness nonlinearity of the soil, which is essential in the accurate simulation of seismic problems

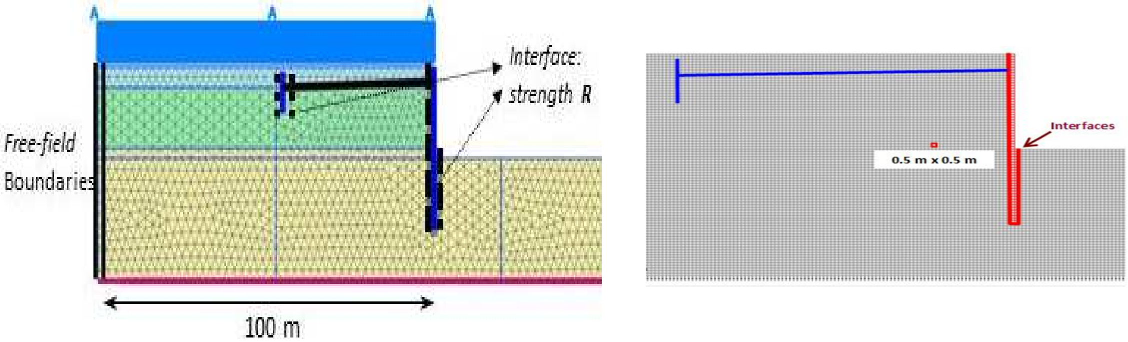


**Figure 2.** Detail of the FE mesh used in the analysis with PLAXIS and ABAQUS

*ABAQUS*: The FE domain shown in Fig. 2 is discretized in ABAQUS using quadrilateral solid plane-strain fine elements 0.5 x 0.5 $m^2$, capable of transmitting without bias the wave frequencies of significance. Interface between wall and soil is tension-less and frictional; it is modeled with special elements that allow both separation and sliding, the latter controlled by coefficients of friction $\mu$. To capture radiation damping normal and shear viscous elements $\rho V_S$ and $\rho V_P$ (per unit area) are placed at the vertical boundaries between the soil domain and the vertical free-field column which is introduced in order to have proper transmission of up-coming waves (avoiding the box effect).

The soil materials were simulated by a model developed at NTUA by Gerolymos & Gazetas (2006) and Anastasopoulos et al (2011). Utilized here by means of a user subroutine, it models the nonlinear soil inelasticity through a simple kinematic hardening with Von Mises failure criterion and an associative flow rule. The evolution law consists of two components: a nonlinear kinematic hardening component describing the translation of the yield surface in stress space, and an isotropic hardening component which defines the size of the yield surface as a function of plastic deformation. Details can be found in the related references.

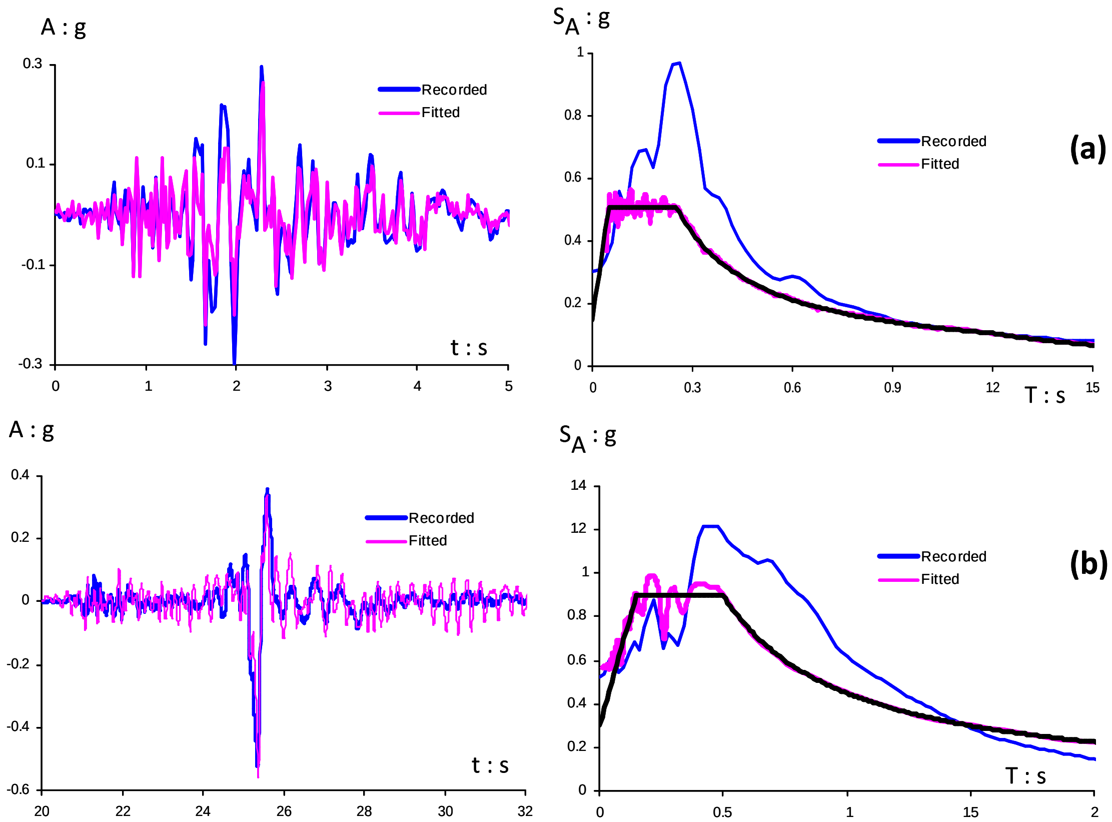


**Figure 3.** Detailed acceleration timehistories (left) of the recorded and fitted ground motions and their response spectra (right) for: (a) the Cogswell Dam motion of Category I, and (b) the TCU 076 of Category II.

**Seismic excitation**

To draw conclusions on the capability of SSP walls to withstand ground shaking in regions of moderate, and very high seismicity, three sets of acceleration time histories were developed:

- Category I: Moderate seismic intensity ground motions with effective ground acceleration 0.15g, corresponding to earthquake events of approximate magnitude M: 5.5 < M < 6.
- Category II: Strong seismic intensity ground motions with effective ground acceleration 0.30g, for earthquake events of magnitude roughly in the range 6 < M < 6.7.
- Category III: Extreme seismic intensity ground motions with effective ground acceleration 0.50g, for earthquake events of magnitude M: 6.7 < M < 7.5.

For each category, three characteristic accelerograms are selected from earthquakes around the world recorded in sites with $V_{S,30} = 500 \div 800$ m/s. This corresponds to EC8 to type B Soil Category (very stiff soil to soft rock). These ground motions are suitably modified in the frequency domain, so that their response spectra fit the appropriate seismic design spectra of EC8. Of course, the design spectra of other Seismic Codes could be used instead of EC8. Such spectrum–compatible accelerograms constitute the free-field "Soil-B-outcrop" motions. Fig. 3 illustrates two examples of originally recorded accelerograms and the fitted motions along with their response spectra.

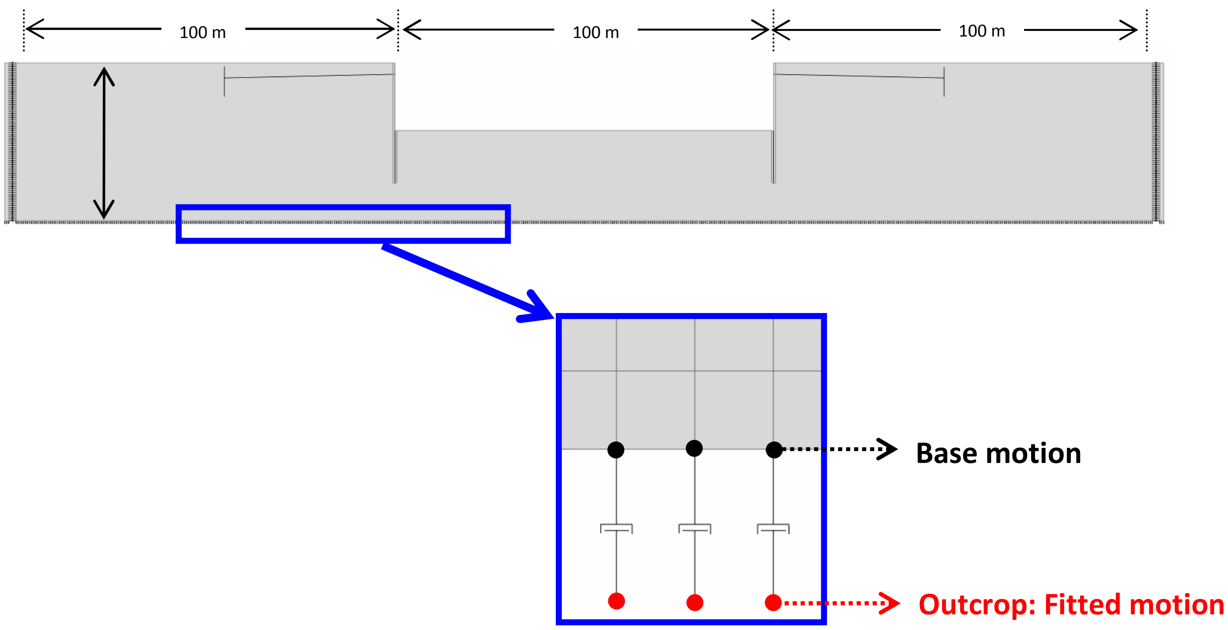


**Figure 4.** The outcrop design motions are imposed at the bottom of vertical dashpots which are placed at the base of the model.

An additional operation is needed to develop the excitation to be input at the fixed base of the retaining system: the difference between outcrop and base motion has to be taken into account. This can be done in a variety of ways. The one utilized here is the classical one : the Soil-B-outcrop motion is input not directly at the base of the model, but through a series of continuously-distributed shear dashpots of a constant impedance $\rho V_s$ , in which $V_s$ is the shear wave velocity of Soil B and $\rho$ is the soil density (Fig.4). The method of applying viscous dampers along boundaries is employed by numerous researchers worldwide as the most appropriate for absorbing reflecting waves and therefore simulate adequately radiation damping

[Bao et al (2012), Chang & Nghiem (2010), Jingbo et al (2006), Nielsen (2006), Hashash & Park (2002), Deeks & Randolph (1994), Kausel (1988), Wolf (1986), Chow (1985), Kunar & Rondriguez-Ovejero (1980)]. Conservatively, we assumed $V_s$ to be equal to 800 m/s.

Fig. 5 compares the two design target spectra, the corresponding spectra of two fitted "rock-outcrop" motions, and the spectra of the resulting "base" motions (accounting for a "rock" shear wave velocity of 800 m/s). Two particular fitted records, Cogswell and Chavriata are shown, corresponding to effective ground accelerations of 0.15 g and 0.50 g, respectively. Note that the fitting to the target spectra was not perfect—this was done deliberately, so as to preserve as much as possible the natural features of the records.

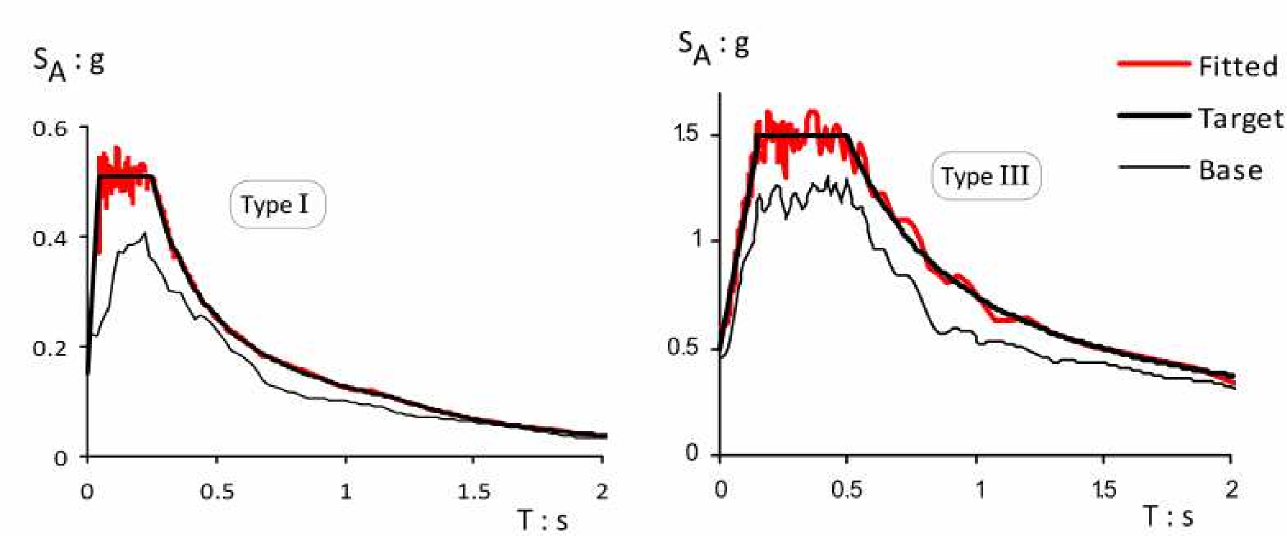


**Figure 5.** Comparison of the "rock outcrop" target and fitted spectra, with the computed "base" motion spectra

**RESULTS**

Typical analysis results are portrayed in Figs. 6-7. In Fig. 6 the deformed shape of the systems with superimposed the contours of plastic strain magnitude are given for two reference cases: one from Category I and one from category III. The snapshots are taken at the time of maximum thrust on the main wall.

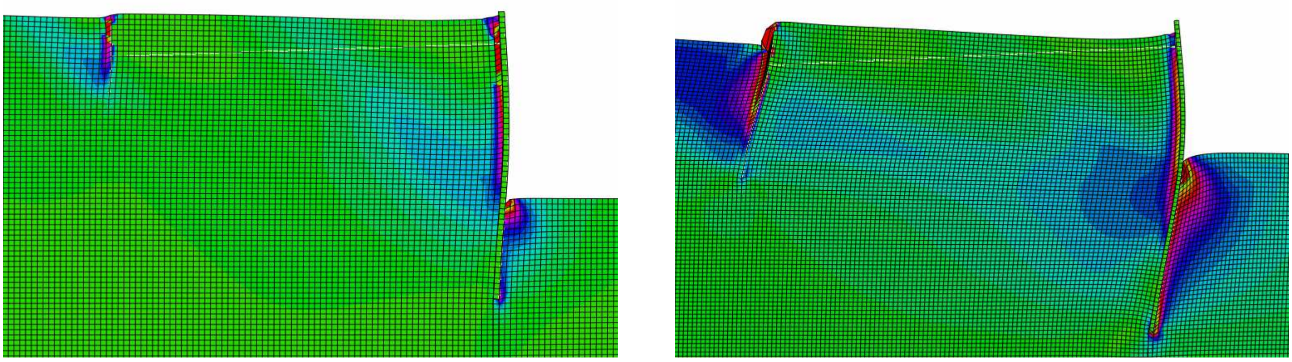

**Figure 6.** Deformed shape with superimposed contours of plastic deformations (PEMAG) for Types I and III excitation. [Deformation Scale Factor = 5]

For Type I, we notice the intense plastic deformations in two regions: in the passive side (in front) of the wall near the mudline, and on active (back) side of the anchor wall. The active wedge on the back side of the wall itself has just begun to form, with smaller plastic strain, and it has almost reached the surface at a clear distance from the anchor. No indication that passive-type strains have ever began to develop in front of the anchor wall; therefore the anchoring system is more than just adequate. Shortening its distance would be quite feasible.

For Type III, the plastification of soil is now by far more extensive, and the deformation of the system larger. Moreover, the “active” failure surface seems to be forming at a much reduced angle with respect to the horizontal and has already interfered with the passive wedge of the anchor. The only danger stems from the SSP wall itself, which is heavily strained and displaced.

Fig. 7 plots the distributions with depth of the bending moments of the main SSP wall, for the Type I and III motions respectively. The results for the Type I motion highlight the conservatism in designing such systems with simplified methods, since significantly larger values were predicted than those computed by both FE codes. From the FE results it is furthermore evident that the choice of the constitutive model for the soils has little effect mainly in the computed structural distress.

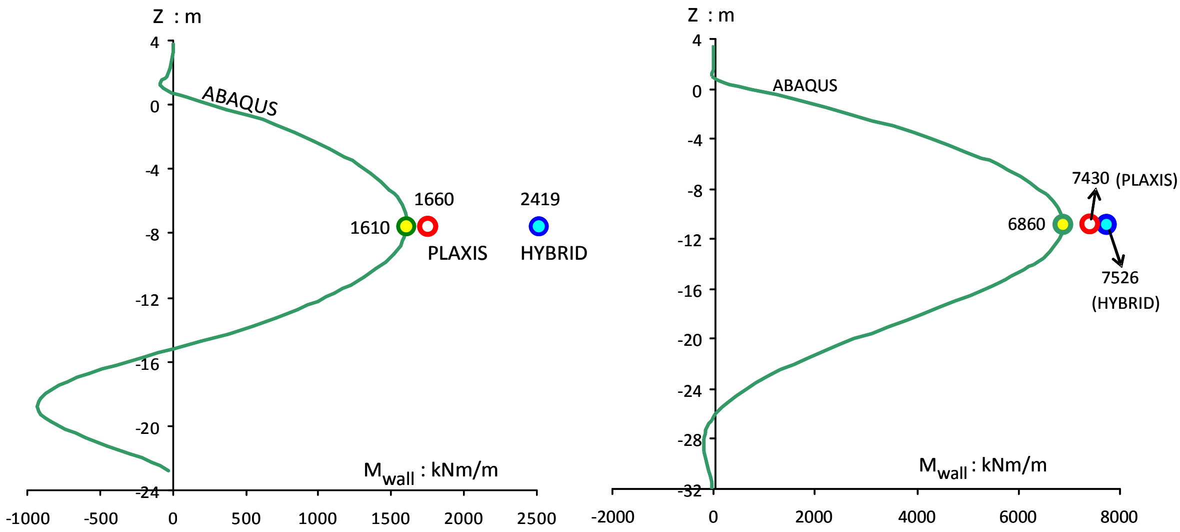


**Figure 7.** Comparison of bending moments of the main SSP wall for Type I and III excitations respectively, obtained with the two FE codes (at the time of maximum soil thrust) and a hybrid MO-based method (note: for the Type III motion the ultimate state reached at α = 0.40g).

As for the results under the strong motion we observe a substantial increase in the bending moments, with the maximum value lying between 6800 and 7500 kNm/m, thus approaching—but not reaching—the ultimate moment capacity of the particular SSP.

It should be noted, however, that the limit state using this simplified method was reached at α = 0.40 g, contrary to the α = 0.50 g used as the effective acceleration at the rock outcrop in the FE analyses. Therefore, the respective results (from FEM and hybrid method) are not directly comparable. It was nevertheless deemed useful to be presented alongside, in order to highlight the limitations and applicability of each method.

## CONCLUSIONS

The paper presents results from a case study of the seismic response of a deep anchored steel sheet-pile (SSP) wall supporting 18 m of soil. It is shown that the simplified methods based on the Mononobe-Okabe method typically used in design practice may lead to very conservative results regarding the bending distress of the wall, since it is impossible to capture the dynamic interaction between soil, SSP wall, and anchor wall. The development of regions of concentrated plastic deformation (surrogates of Coulomb sliding surfaces) however cannot be represented in such models even when nonlinear p–y type of “springs” are used. The available well established FE codes can, on the other hand, be used to estimate realistically the distress and deformation demands of the SSP-tie rod-anchor wall system. By means of these advanced methods it is demonstrated that the response of the SSP wall can be quite satisfactory, for both moderate and very high intensity motions. Numerical analysis is thus recommended and especially when the performance of such systems is evaluated within a Performance-based design framework.

## REFERENCES


*ABAQUS Documentation* 2011, Dassault Systèmes, Providence, RI, USA.

Agbabian Associates. *Seismic Response of Port and Harbor Facilities* 1980, Report P80-109-499, El Segundo, California.

Al Atik L, Sitar N. Seismic Earth Pressures on Cantilever Retaining Structures. *J Geotech Geoenviron Eng* ASCE 2010, 136(10), 1324-1333.

Anastasopoulos I, Gelagoti F, Kourkoulis R, Gazetas G. Simplified constitutive model for simulation of cyclic response of shallow foundations: validation against laboratory tests. *J Geotech Geoenviron Eng* ASCE 2011, 137(12): 1154–1168.

Bao H, Hatzor YH, Huang X. A new viscous boundary condition in the two-dimensional discontinuous deformation analysis method for wave propagation problems, *Rock Mech Rock Eng*, 2012, **45**: 919–928.

Chang NY, Nghiem HM. Viscous damping for time domain finite element analysis, *Fifth International Conference on Recent Advances in Geotechnical Earthquake Engineering and Soil Dynamics and Symposium in Honor of Professor I.M. Idriss*, 2010, San Diego, California, Paper N° 2.15

Chow YK. Accuracy of consistent and lumped viscous dampers in wave propagation problems, *International Journal For Numerical Methods In Engineering*, 1985, **21**: 723-732.

Dakoulas P, Gazetas G. Insight into Seismic Earth and Water Pressures against Caisson Quay walls. *Géotechnique* 2008, 58 (2), 95 – 111.

Deeks AJ, Randolph MF. Axisymmetric time-domain transmitting boundaries, *Journal of Engineering Mechanics*, 1994, 120(**1**): 25-42.

Dennehy KT. *Seismic Vulnerability, Analysis, and Design of Anchored Bulkheads*. Ph.D Thesis 1985, Rensselaer Polytech. Inst., Troy NY.

Ebeling RM, Morrison EE. *The Seismic Design of Waterfront Retaining Structures*. Technical Report ITL-92-11 1992, Washinghton DC, US Army Corps of Engineers.

Gazetas G, Dakoulas P, Dennehy K. Empirical Seismic Design Method for Waterfront Anchored Sheetpile Walls. *Design and Performance of Earth Retaining Structures* ASCE 1990, 232-250.

Gerolymos N, Gazetas G. Static and dynamic response of massive caisson foundations with soil and interface nonlinearities—validation and results. *Soil Dyn Earthq Eng* 2006, 26(5): 377–394.

Hashash YMA, Park, D. Viscous damping formulation and high frequency motion propagation in non-linear site response analysis, *Soil Dynamics and Earthquake Engineering*, 2002, **22**: 611–624.

Hayashi S, Katayama T. Damage to Harbor Structures by the Tokachioki Earthquake. *Soils and Foundations* X 1970, 83-102.

Japan Society of Civil Engineers. Earthquake Resistant Design of Quaywalls and Piers in Japan. *Earthquake Resistant Design for Civil Engineering Structures, Earthquake Structures and Foundations in 1980*, 31-85.

Jingbo L, Yixin D, Xiuli D, Zhenyu W, Jun W. 3-D viscous-spring artificial boundary in time domain, *Earthquake Engineering and Engineering Vibration*, 2006, 5(**1**): 93-102.

Kausel E. Local transmitting boundaries, *Journal of Engineering Mechanics*, 1988, 114(**6**): 1011-1027.

Kawakami F, Asada A. Damage to the Ground and Earth Structures by the Niigata Earthquake of June 16, 1964. *Soils and Foundations* VI 1966, 14-60.

Kunar RR, Rodriguez-Ovejero L. A model with non-reflecting boundaries for use in explicit soil-structure interaction analyses, *Earthquake Engineering and Structural Dynamics*, 1980, **8**: 361-374.

Nielsen AH. Absorbing boundary conditions for seismic analysis in ABAQUS, *ABAQUS Users' Conference*, 2006, pp. 359-376.

*PIANC 2001*. Seismic Design Guidelines for Port Structures. Tokyo: A.A. Balkema.

*PLAXIS 2012*. PLAXIS 2D Anniversary Edition. 2600 AN Delft, The Netherlands.

Richards R, Elms D. Seismic Behavior of Gravity Retaining Walls. *J Geotechnical Engineering Div*. ASCE 1979, 105.

Towhata I, Ghalandarzadeh A, Sundarraj K, Vargas-Monge W. Dynamic Failures of Subsoils Observed in Water-Front Areas. *Soils Foundations (Special Issue on Geotechnical Aspects of the January 17, 1995 Hyogoken-Nambu Earthquake)* 1996, 149-160.

Wolf JP. A comparison of time-domain transmitting boundaries, *Earthquake Engineering and Structural Dynamics*, 1986, **14**: 655-673.